ONERA

THE FRENCH AEROSPACE LAB

F I N A L   R E P O R T

Cold atom gravimetry airborne test in Iceland

Authors : A. Bresson ; N. Zahzam ; Y. Bidel ;
A.V. Olesen ; R. Forsberg

PHYSICS INSTRUMENTATION ENVIRONMENT SPACE

ONERA

THE FRENCH AEROSPACE LAB

PHYSICS INSTRUMENTATION ENVIRONMENT SPACE

Final Report N° RF 1/27274 DPHY

June 2018

Cold atom gravimetry airborne test in Iceland

Written by :

A. Bresson ; N. Zahzam ; Y. Bidel ; A.V. Olesen (DTU Space) ; R. Forsberg (DTU Space)

Verified by :

Alexandre Bresson, Head of Laser Sources and Metrology Unit

Approved by :

Deputy Director of
Physics Instrumentation Environment spacE
O. Le Traon

IDENTIFICATION CARD of ONERA REPORT N° RF 1/27274 DPHY

Issued by : **PHYSICS INSTRUMENTATION ENVIRONMENT SPACE**	Contracting Agency : **DTU Space**	Contract Number : **DPhIEE-PTF-17-26 DTU Approval of ONERA proposal - April 16, 2017**
		Date : **June 2018**

Title :	**Cold atom gravimetry airborne test in Iceland**

Author(s) : **A. Bresson ; N. Zahzam ; Y. Bidel ; A.V. Olesen ; R. Forsberg**

SECURITY CLASSIFICATION : Civil Title : UNPROTECTED ID Card : UNPROTECTED Report : UNPROTECTED	Timing Classification Off Title : Without object ID Card : Without object Report : Without object

Abstract :

This report describes the results of the ESA Cold Atom interferometry airborne test campaign in Iceland, April 2017, as a follow-up activity to the major ESA CryoVEx-KAREN validation campaigns in Arctic Canada, Greenland, and Svalbard.

The test flights of the ONERA cold atoms instrument GIRAFE, modified for airborne measurements, was carried out as a follow-up opportunity to the main CryoVEx campaign, using the same aircraft, and the same supporting navigation, positioning equipment and power racks of DTU Space. The campaign took place across Iceland, using a Twin Otter DHC-6 from Norlandair, Akureyri, and consisted of repeat flights in northern Iceland and a small demonstration survey pattern over the Vatnajokull ice cap.

The Iceland flight campaign was the first ever airborne gravity survey using cold atom matter-wave gravimetry, and given the challenges of installation of equipment, and turbulent flights over rugged topography a highly successful demonstration campaign. The estimated accuracy of the airborne cold atom survey was 2 mGal in an absolute sense, based on both repeat flights and cross-over data, as well as comparisons to upward continued ground gravity data.

The present report is separate part (Vol. 2) of the Final Report of the main ESA 2017 CryoVEx campaign.

Key words :
GRAVIMETRIE AÉROPORTÉE ; INTERFEROMETRIE ATOMIQUE ; GRAVIMETRE ABSOLU ; ATOME FROID

ONERA
THE FRENCH AEROSPACE LAB

DISTRIBUTION LIST of ONERA REPORT N°RF 1/27274 DPHY

Distribution of report

• Outside ONERA :

DTU Space	A. V. Olesen, R. Forsberg	2 ex.
CNAM	M. Cadoret (+ version électronique)	1 ex.

• Inside ONERA :

DPHY/SLM	A. Bresson, N. Zahzam, Y. Bidel (+ version électronque)	3 ex.
DPHY/SLM	C. Blanchard (+ version électronique)	1 ex.
DIST	Documentation	1 ex.

Distribution of identification card

• Inside ONERA (with link to full text) :

DPHY/DAdj	O. Le Traon	1 ex.
DPHY/D	J.-F. Roussel	1 ex.
DPHY/AOP	J.-P. Carayon	1 ex.
DPHY/SLM	A. Bresson, N. Zahzam, Y. Bidel	3 ex.
DPHY/SLM	C. Blanchard	1 ex.
	Systematic distribution : DSP, DTP, DAI	3 ex.

Cold atom gravimetry airborne test in Iceland

**A part of the ESA CryoVEx-KAREN Arctic field campaign 2017
ESA contract number 4000120131/17/NL/FF/mg**
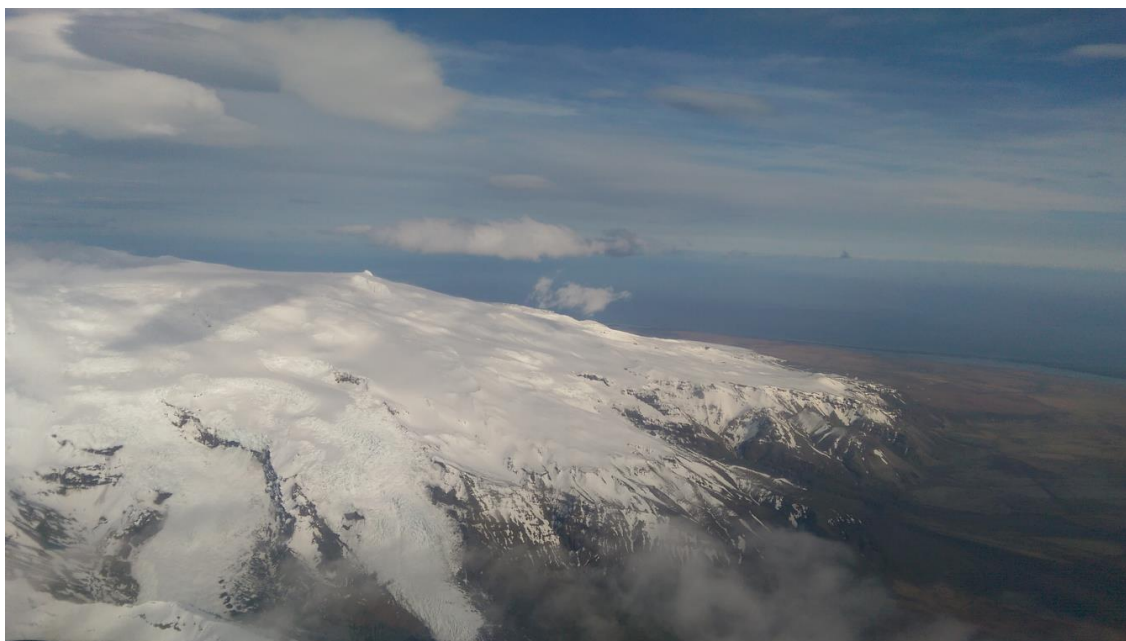
**Final Report
May 2018**

**A. Bresson, N. Zahzam, Y. Bidel
ONERA, France**

**A. V. Olesen and R. Forsberg
National Space Institute, Denmark**

RF 1/27274 DPHY

JUNE 2018

ESA STUDY CONTRACT REPORT

ESA CONTRACT NO 4000120131/17/NL/FF/mg	**SUBJECT** Technical Support for the 2017 Airborne		**CONTRACTOR** DTU Space
ESA CR No	**STAR CODE**	**No of volumes: 2 This is Volume No** 2 (partial report)	**CONTRACTORS REFERENCE** Cold Atoms 2017

ABSTRACT

This report describes the results of the ESA Cold Atom interferometry airborne test campaign in Iceland, April 2017, as a follow-up activity to the major ESA CryoVEx-KAREN validation campaigns in Arctic Canada, Greenland, and Svalbard.

The test flights of the ONERA cold atoms instrument GIRAFE, modified for airborne measurements, was carried out as a follow-up opportunity to the main CryoVEx campaign, using the same aircraft, and the same supporting navigation, positioning equipment and power racks of DTU Space. The campaign took place across Iceland, using a Twin Otter DHC-6 from Norlandair, Akureyri, and consisted of repeat flights in northern Iceland and a small demonstration survey pattern over the Vatnajokull ice cap.

The Iceland flight campaign was the first ever airborne gravity survey using cold atom matter-wave gravimetry, and given the challenges of installation of equipment, and turbulent flights over rugged topography a highly successful demonstration campaign. The estimated accuracy of the airborne cold atom survey was 2 mGal in an absolute sense, based on both repeat flights and cross-over data, as well as comparisons to upward continued ground gravity data.

The present report is separate part (Vol. 2) of the Final Report of the main ESA 2017 CryoVEx campaign.

The work described in this report was done under ESA Contract. Responsibility for the contents resides in the author or organisation that prepared it.

NAMES OF AUTHORS

A. Bresson, N. Zahzam, Y. Bidel, A. V. Olesen and R. Forsberg

NAME OF ESA STUDY MANAGER Tania Casal Mission Science Division Validation Campaigns – ESTEC	**ESA BUDGET HEADING**

ONERA
THE FRENCH AEROSPACE LAB

GEN-F157-6

CONTENTS

ONERA
THE FRENCH AEROSPACE LAB

1. INTRODUCTION

This document is the report of the gravity airborne campaign with the cold atom gravimeter GIRAFE developed at ONERA. This campaign was done in collaboration between ONERA and DTU and was cofunded by ONERA, ESA and DTU.

The precise knowledge of Earth's gravity field is of major importance in several domains. In geodesy, it is essential for describing the continental and sea surface topography, since the geoid, an equipotential surface of gravity, is used as a height reference. In geophysics, gravity measurements provide information on the underground mass distribution and its variations. They allow thus mapping tectonic structure [1], studying volcano [2] and earthquake [3], monitoring ice melting [4], measuring water storage variation [5] or exploring oil, gas and mineral [6]. The knowledge of gravity field is also essential in inertial navigation as navigation algorithms need a precise gravity model [7].

The Earth's gravity field can be measured from space by using for example satellite to satellite tracking methods[8],[9] or satellite borne gravity gradiometer [10],[11]. Nevertheless, these methods lead to gravity maps with a spatial resolution limited to 100 km. For over sea areas, resolutions of 16 km can be reached by using radar satellite altimetry [1]. Higher spatial resolutions can only be obtained with airborne or ship borne measurements. Until now, these surveys were carried out with relative sensors which only measure variation of gravity and which suffer from drift. For a gravity survey, one needs thus to go regularly to a reference point where the gravity is known or where there is a static absolute gravimeter. Therefore, the use of a relative gravimeter has important operational constraints which increase the time and the cost of gravimetry survey and has measurement errors due to calibration and drift estimation. The use of an absolute gravimeter would thus be of great interest but until now these instruments can only work in static conditions. Only one feasibility study done with a modified FGL gravimeter on an aircraft [12] can be found in the literature.

At ONERA, we are developing since 10 years an onboard absolute gravimeter based on matter wave interferometry named GIRAFE. This instrument is based on the acceleration measurement of a free falling gas of ultra cold atoms with atom interferometry [13]. This technology has been developed since three decades and has allowed testing fundamental physics [14][15], measuring fundamental physics constants [16][17] and measuring with high precision gravity [18][19][20][21] , gravity gradient [22][23] and rotation [24][25][26]. Most of these works consist in laboratory experiments but more and more atom interferometer are performed outside laboratory environment such as in a truck [27], an elevator [28], a zero-G airplane [29][30], a dropped tower [31] or a sounding rocket [32]. Concerning gravimeter, matter wave sensors have now better or equal performances than classical absolute gravimeters [18][19][20][21] and start to be commercialized. Some attempts have been made to use these technologies in a moving platform but, until now, only limited demonstrations could be found in the literature. In ref. [27], mobile gravity gradient measurements are reported in a truck moving at only 1 cm/s. In ref. [29] and [30], acceleration measurements in a zero-G plane are reported but no gravity measurements were performed. In ref. [28], low precision gravity measurements are reported in a moving elevator.

We demonstrated recently in collaboration with SHOM absolute gravity measurements from a ship with a sensor based on atom interferometry [33]. Despite rough sea conditions, we obtained precisions below 1 mGal (10^{-5} m.s^{-2}). The atom gravimeter was also compared with a commercial spring gravimeter and showed better performances.

Here, we report the test of this gravimeter in an airplane. This work was done in collaboration with DTU. To our knowledge, it is the first time that a cold atom gravimeter has been tested in an airplane for gravimetry survey.

ONERA
THE FRENCH AEROSPACE LAB

2.   DESCRIPTION OF THE COLD ATOM GRAVIMETER

The gravimeter (see Figure 1) is composed of an atom sensor which provides an absolute measurement of the acceleration, a gyro-stabilized platform which maintains the accelerometer aligned with the gravity acceleration despite angular movements of the carrier and systems which provide the lasers and microwaves needed to the atom sensor and perform data acquisition and processing.
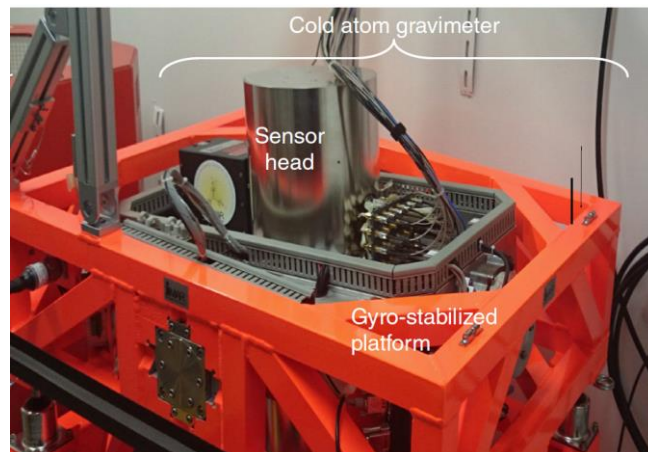
Figure 1- Picture of the cold atom gravimeter GIRAFE (sensor and platform).

The atom accelerometer is similar to the one described in reference [28]. The test mass is an ultracold gas of rubidium 87 atoms. It is produced from a magneto-optical trap loaded from a background vapor. After 20 ms of trap loading, a stage of optical molasses and a microwave selection, we obtain a cloud of one millions atoms in the magnetic field insensitive ground state F=1, m_F=0 and at a temperature of 1.9 µK. The acceleration of the free falling cloud of ultracold atoms is then measured by light pulse atom interferometry. For that, we use a Mach-Zehnder type atom interferometer consisting of a sequence of three equally spaced Raman laser pulses of duration 10, 20 and 10 µs which couple the two hyperfine ground states F=1, m_F=0 and F=2, m_F=0. The two counter-propagating laser beams addressing the Raman transition are obtained with a phase modulated laser at 6.8 GHz retro-reflected on a mirror [34]. In this interferometry sequence, the first pulse acts as a matter wave beam splitter, the second one acts as a mirror and the last one recombines the matter waves (see Figure 2). The phase shift at the output of the interferometer is equal to $\phi = (k_{eff}.a-\alpha)T^2$ where $k_{eff} \simeq 4\pi/\lambda$, λ the laser wavelength, T the time delay between Raman laser pulses, a the acceleration of the atoms along the direction of the laser beam and α the rate of the radiofrequency chirp applied to the 6.8 GHz frequency in order to compensate for the linearly increasing Doppler shift induced by the acceleration of the atoms. The interference signal is then obtained by measuring the population of atoms in the two hyperfine states corresponding to the two output ports of the interferometer. This measurement is obtained by a fluorescence method. The proportion P of atoms in the state F=2 after the atom interferometer sequence can be written as $P = P_m - C/2 \cos(\phi)$ where P_m is the offset of the fringe and C is the contrast which is typically equal to 0.3 for our sensor. Two different falling distances of 14 mm and 42 mm are possible in our sensor, leading to a maximum half interrogation time of respectively T = 20 ms and T = 39 ms and to a repetition rate of 10 Hz and 7 Hz. The long falling distance is used for static measurements and the short falling distance is more adapted to measurements in a moving vehicle.

The output P of the atom sensor is proportional to the cosine of the acceleration with a period equal to $\lambda/(2T^2)$. For T = 20 ms, this period is equal to 10^{-3} m. s^{-2} and is small compared to typical variations of acceleration in a moving vehicle. There is, therefore, an ambiguity to determine the acceleration from the measurement of the atom sensor. Many values of acceleration are possible for a given value of the output of

ONERA

THE FRENCH AEROSPACE LAB

the atom sensor. To overcome this limitation, we combine the atom sensor with a classical accelerometer. This kind of method has already been successfully implemented in laboratory environment to measure the gravity acceleration [35][36] and in a free falling (zero-G) plane for acceleration measurements [29]. Here, we implement a new robust combination scheme of the atom accelerometer with a force balanced accelerometer (Qflex from Honeywell). The classical accelerometer is used to give a first rough estimation of the acceleration in order to determine which value of acceleration corresponds to the signal of the atom sensor. The classical accelerometer is also used to measure the acceleration during the measurement dead times of the atom sensor which occur during the cold atoms preparation and during the detection. The filling of the measurement dead times is very important because otherwise vibrations at the repetition rate of the atoms sensors and its multiple can cause an important degradation of sensitivity due to aliasing effect.
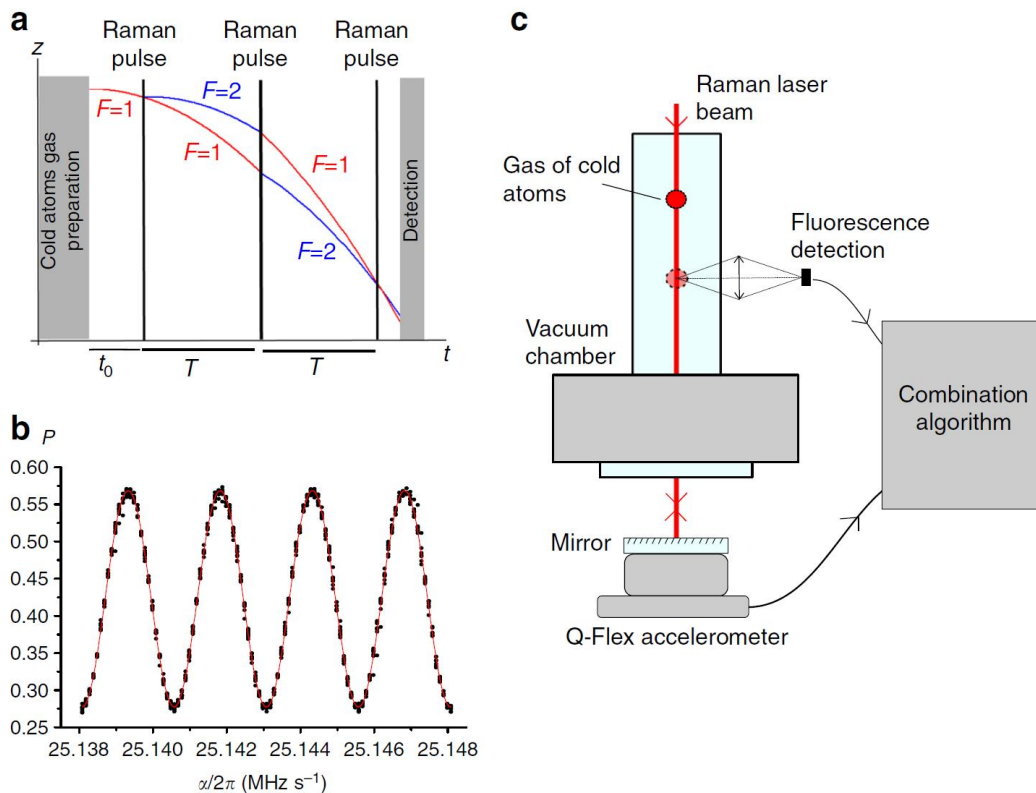
*Figure 2 - Principle of the atom accelerometer. **a** Temporal sequence. **b** Typical interference fringes acquired in static condition for T = 20 ms. **c** Setup of the cold atom accelerometer.*

This atom accelerometer has been implemented in a compact housing consisting of a cylinder of 22 cm diameter and 52 cm height. It is composed of a vacuum chamber made of glass in which the atoms are produced and interrogated, magnetic coils, optics for shaping all the laser beams and collecting the fluorescence of the atoms, two layers of mu-metal for shielding the external magnetic field and classical accelerometers. This sensor is integrated in a two axes stabilized gimbaled platform made by IMAR. The platform is stabilized using an integrated inertial measurement system and maintains the sensor head aligned with the gravity acceleration with a precision of 0.1 mrad. The lasers needed for the sensor are obtained using a compact frequency doubled telecom fiber bench [37] which is compatible with onboard environment.

ONERA

THE FRENCH AEROSPACE LAB

3. CAMPAIGN PREPARATION

3.1. Airborne environment

The gravimeter GIRAFE has been designed for marine ship borne environment. However, airborne environment in which we would like to test the gravimeter is different from ship borne environment. The instrument is subject to stronger vibrations in an airplane than in a boat. In boat, the acceleration spectrum is a peak centered at the swell frequency (~ 0.1 Hz) and in the plane the acceleration spectrum is more distributed (see Figure 3).

Airborne environment   *Ship borne environment*
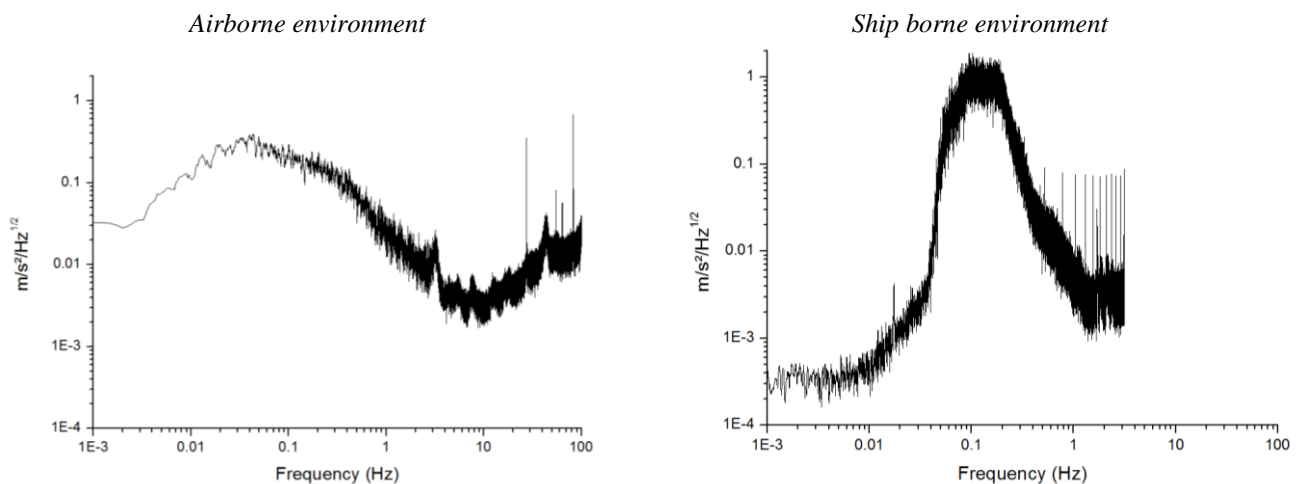
Figure 3 – Comparison of the acceleration spectrum in airborne and ship borne environment. The airborne acceleration spectrum comes from a DTU campaign in Antartica with a Twin-Otter during a non-turbulent period. The ship borne acceleration spectrum comes from acceleration measurement in a 80 m boat (Beautemps-Beaupré).

In order to adapt and pre-test our gravimeter to airborne conditions, we improved the model of the classical accelerometer at high frequency, we characterized the vibration isolation of the platform and finally we tested the gravimeter with a motion simulator (hexapod) simulating airborne environment. All this tasks will be detailed in next parts.

We checked also the electromagnetic-compatibility of the gravimeter with the airplane. For that, we checked that it is possible to hear VHF the communications from the Orly airport located at 20 km from our laboratory. The test was done with a VHF receiver located next to the gravimeter.

3.2. Improvement of the force balanced accelerometer model for high frequency vibration

The hybridization of the atom and the classical accelerometer is working well if the difference between the acceleration given by the atom accelerometer and the classical accelerometer is smaller than a period of the atom accelerometer signal $\lambda/(2T^2)$, 100 µg pour T=20 ms. For boat environment, we supposed that the transfer function of the classical accelerometer is equal to 1. This was a good approximation because the frequency cut off of the classical accelerometer is around 1 kHz and the gravimeter was not subjected to a high level of high frequency vibration. However, in an airplane, the gravimeter is subject to stronger vibration and the transfer function of the classical accelerometer has to be compensated in order to optimize the performance of the gravimeter.

The classical accelerometer that we use is forced balanced accelerometer made by Honeywell (Qflex) and we did not find in the datasheet and in the literature the transfer function of the accelerometer. We thus

ONERA
THE FRENCH AEROSPACE LAB

estimated empirically the transfer function of the accelerometer. For that, we model the transfer function by a damped harmonic oscillator:

$$\hat{h}_{FB}(\omega) = \frac{\omega_0^{\,2}}{\omega_0^{\,2} - \omega^2 + i \cdot \Gamma \cdot \omega}$$

We estimated the parameter Γ and ω_0 by minimizing the difference between the estimated acceleration from the classical accelerometer and the atom accelerometer measurement in presence of high frequency vibration. The values obtained are:

$$\omega_0 = 1.57 \cdot 10^3 \text{ s}^{-1}$$
$$\Gamma = 2.42 \cdot 10^3 \text{ s}^{-1}$$

3.3.   Characterization of the vibration isolator of the platform

The gyro-stabilized platform of the gravimeter is equipped of 8 isolators to damp vibrations coming from the vehicle (see Figure 4).

Figure 4 - Vibration isolators of the platform.

Because the level of vibration is high in an airborne environment, we undertook to characterize precisely the vibration isolators of the platform. For that, we excited in vibration the gravimeter with a white noise thanks to the motion simulator. Then we recorded the acceleration measured on the base plate of the gravimeter and the acceleration measured inside the sensor head. The transfer function of the vibration is finally obtained by dividing the acceleration spectrum measured in the sensor head and the acceleration spectrum measured on the base plate (see Figure 5). The transfer function obtained is behaving like a second order low pass filter with a resonant frequency at 12 Hz. We can also remark frequency resonances at 115 Hz and 178 Hz.

ONERA
THE FRENCH AEROSPACE LAB
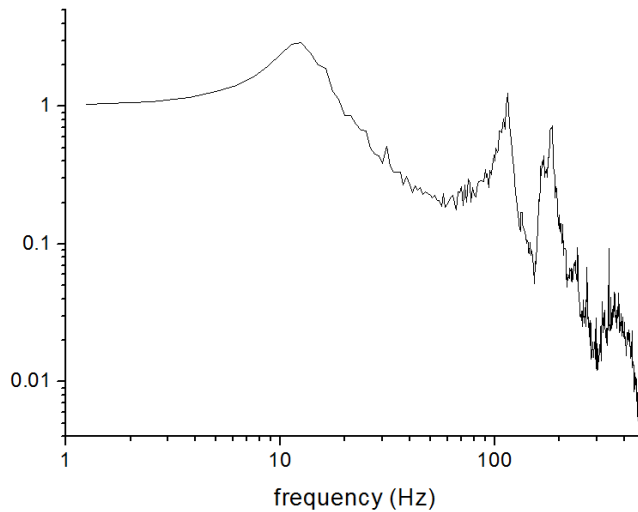
Figure 5 – Measured transfer function of the vibration isolators of the platform.

3.4. Simulation of the airborne environment with a motion simulator

The goal here is to reproduce as well as possible the motion of an airplane with our motion simulator. For that, we took 100 s of IMU data coming from measurements made during a non-turbulent flight by DTU campaign in Antarctica with a Twin-Otter. Then we programed the motion simulator to reproduce the three translations and three rotations measured by the IMU. The translations were high pass filtered at a frequency of 0.2 Hz in order that to have translations in the range of the motion simulator (± 0.18 m).
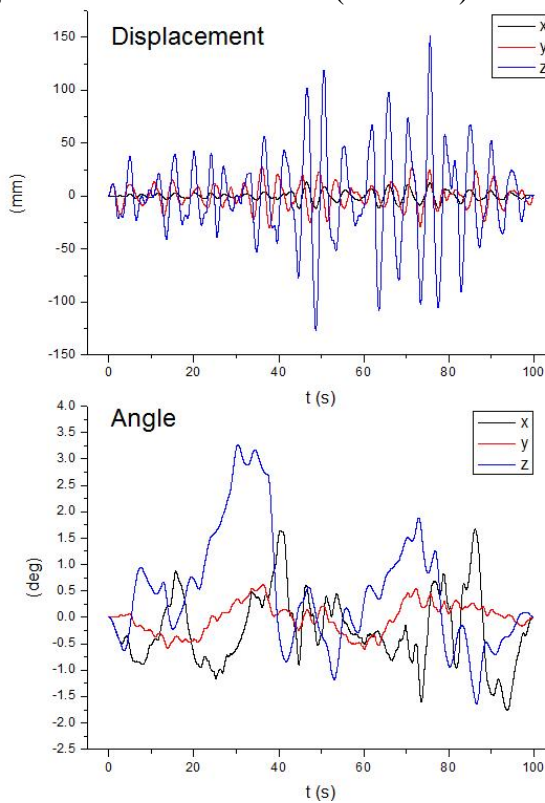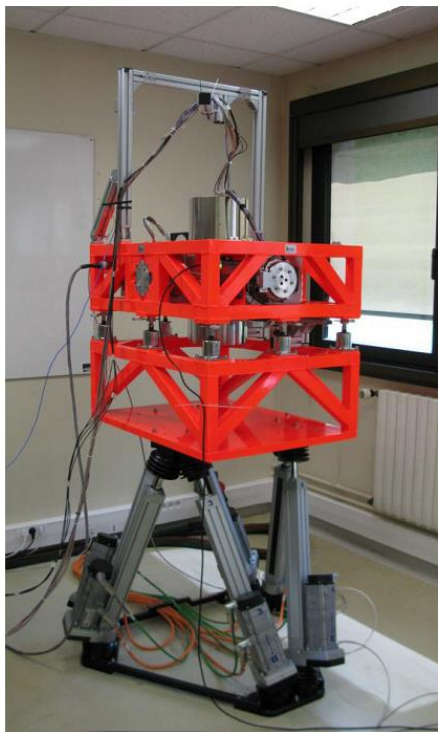
Figure 6 - Simulation of the airborne environment with a motion simulator. Left: picture of the gravimeter on the motion simulator. Right: Movement in translation and rotation (z axis is vertical).

To check the fidelity of simulation, we measured the vertical acceleration on the base plate of the gravimeter and we compared it with the acceleration coming from the IMU of the plane (see Figure 7).
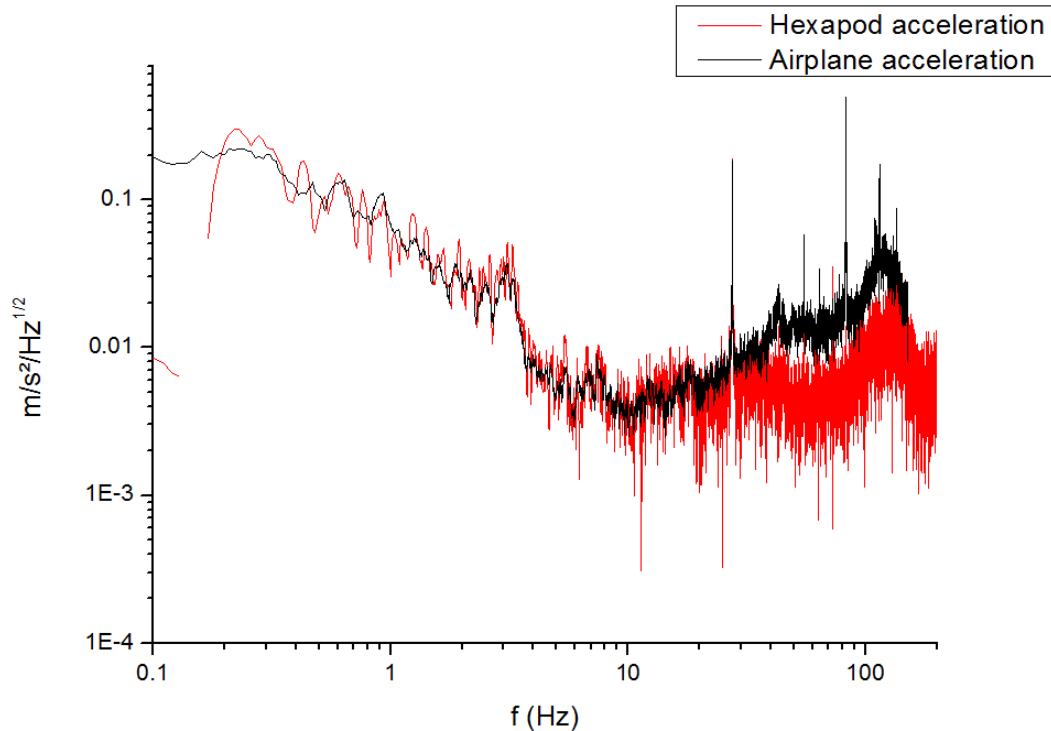
Figure 7 - Comparison of the vertical acceleration obtained with the motion simulator and the acceleration coming from a real flight.

We notice that the motion simulator reproduced well the acceleration spectrum between 0.2 Hz and 20 Hz. The slow motion below 0.2 Hz should not be a problem for our gravimeter but the acceleration above 20 Hz could affect the performance of the gravimeter and specially the acceleration around frequency of 115 Hz which are not filtered by the vibration isolator (see 3.3). To simulate this effect, we use a shaker located next to the gravimeter and we exited at a frequency 115 Hz. Thanks to this method, a vibration level of 40 mg at 115 Hz has been obtained on the base plate of the gravimeter.

We measured gravity while the sensor was subjected to the simulated movement of the plane with the hexapod and to vibrations at 115 Hz with the shaker. The gravity measurements obtained are shown on Figure 8. The gravimeter was subjected to simulated airborne condition during two periods of 1000 s with a break of 1000 s between them. We notice that the mean value of measured gravity has not significantly changed during the period of motion simulation. The rms noise on the filtered gravity measurement is equal to 0.3 mGal during motion and 0.1 mGal during static period. These results are quiet good and similar to the one obtained during marine campaign. This is an important first step validation before the real airborne test.

ONERA

THE FRENCH AEROSPACE LAB
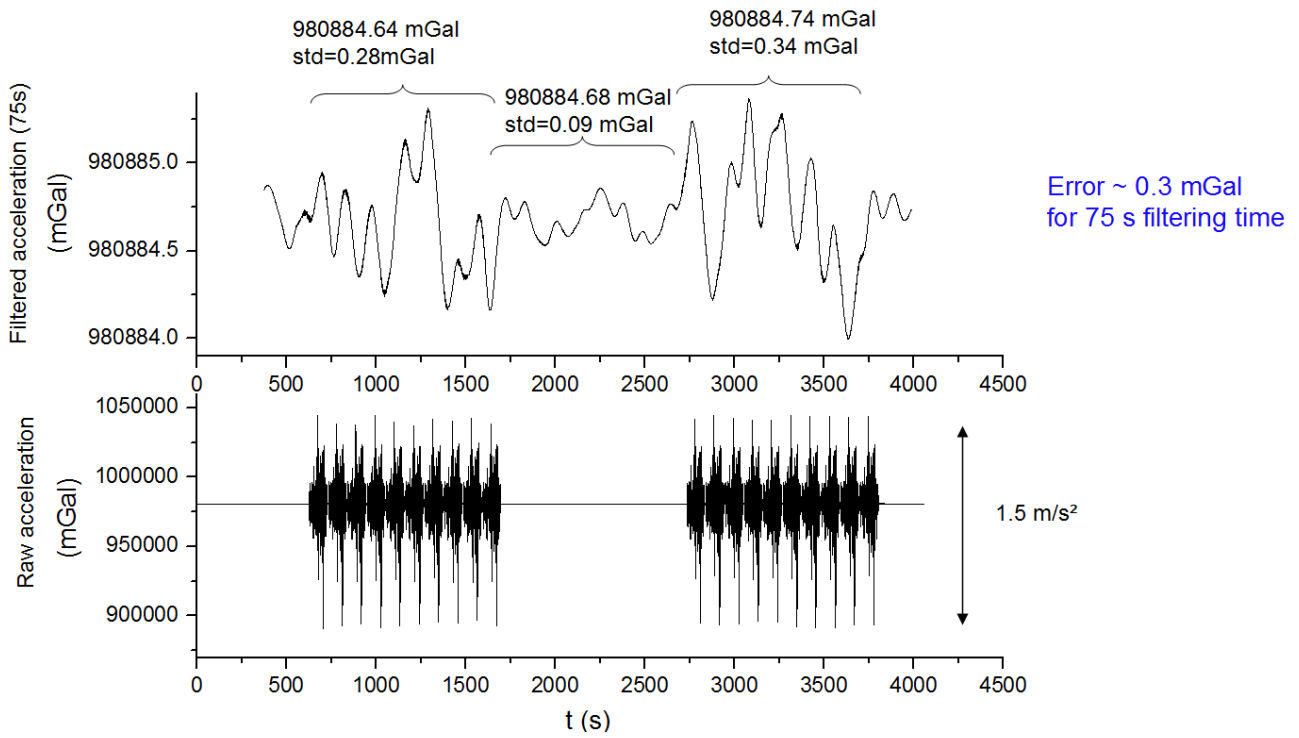
Figure 8 - Gravity measurement during airplane motion simulation. Top: Gravity measurement after a 75 s Bessel low filter of order 4. Bottom: Vertical acceleration measured on the base plate of the gravimeter.

4. STATIC GRAVITY MEASUREMENT IN ICELAND

The gravimeter GIRAFE was transported from Palaiseau (France) to Akureyri (Iceland) by a transport company which used a road transport in a truck from France to Denmark and a ferry from Denmark to Iceland. The transportation lasted one week.

In order to check the proper functioning of the gravimeter after the transport, we performed a static gravity measurement in plane hangar of Akureyri (see Figure 9). We obtained a value of g = 982 337.37 mGal ±0.07 mGal at 99 cm above the ground. This value agrees well with a previous A-10 absolute gravity measurement made in the hangar by DTU Space.

Figure 9 – Static gravity measurement in the airplane hangar in Akureyri.

ONERA
THE FRENCH AEROSPACE LAB

GEN-F157-6

5.   AIRBORNE GRAVITY CAMPAIGN

5.1.   Installation of the gravimeter in the airplane

The gravimeter (sensor and platform) has been fixed in the plane thanks to an adaptation plate build for the purpose. The fixation holes of the plate were drilled only in Akurery in order to match precisely the fixation holes in the plane. The two control cabinets of the gravimeter could not fit in the plane. Thus the racks were disassembled and arranged in 4 small cabinets adapted to the plane provided by DTU.

Figure 10 - Gravimeter packaged for airplane installation. On the front, one can see the four cabinets containing the electronic and laser racks of the gravimeter.

The gravimeter has been then installed in the airplane according to the plan on Figure 11. The wiring between the different racks and the gravimeter is also described on this figure. The platform with the sensor has been installed next to a strapdown relative gravimeter made by IMAR and operated by DTU (see Figure 12).

ONERA

THE FRENCH AEROSPACE LAB
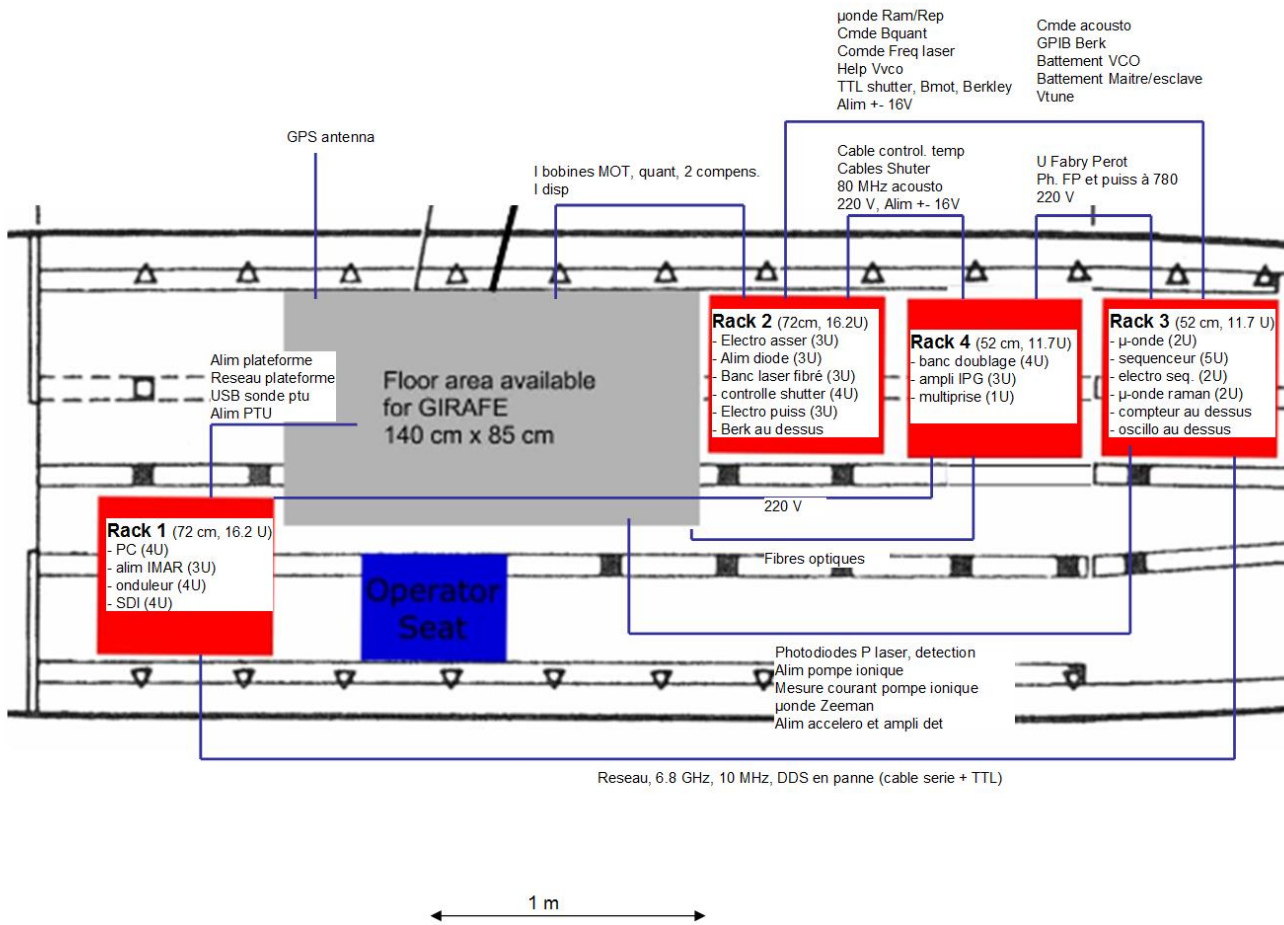
Figure 11 - Plan of installation of the gravimeter in the plane and wiring.

Cold atom gravimeter

Imar gravimeter (IMU)

Figure 12 - Picture of the installation of the gravimeter in the airplane.

ONERA
THE FRENCH AEROSPACE LAB

GEN-F157-6

The gyro-stabilized platform of the cold atom gravimeter needs a GPS antenna. For incompatibility reason, we could not use the GPS antenna of the plane. We thus used our own GPS antenna that was placed on the top of dashboard of the pilots.

The electrical consumption of our gravimeter estimated to 1.4 kW was too high for the available inverter which produces 220 V from the battery on the plane. We lowered the electrical consumption of our gravimeter by replacing the desktop controlling the gravimeter by a laptop and by turning off all non essential equipments: scope, counter and microwave frequency reference. Because we did not use anymore our microwave frequency reference, we had to calibrate our microwave before each flight. Finally, we obtained power consumption compatible with the available inverter.

5.2. Alignment of the gravimeter

After an electrical shutdown, the platform of the gravimeter has to be aligned in order to ensure a perfect alignment with the gravity acceleration. This alignment consists in measuring the acceleration versus the orientation of the platform. The platform is well aligned with the gravity acceleration when the value of acceleration is maximized. The measurements of acceleration versus orientation are reported on Figure 13. The orientations of the platform in static are measured thanks to two horizontal accelerometers located in the sensor head. The orientation corresponding to a measurement axis aligned with the gravity acceleration is obtained by fitting the measurement points by a parabola. With this method, one obtains a precision of 10 µrad below the angular stability of the platform (100 µrad).
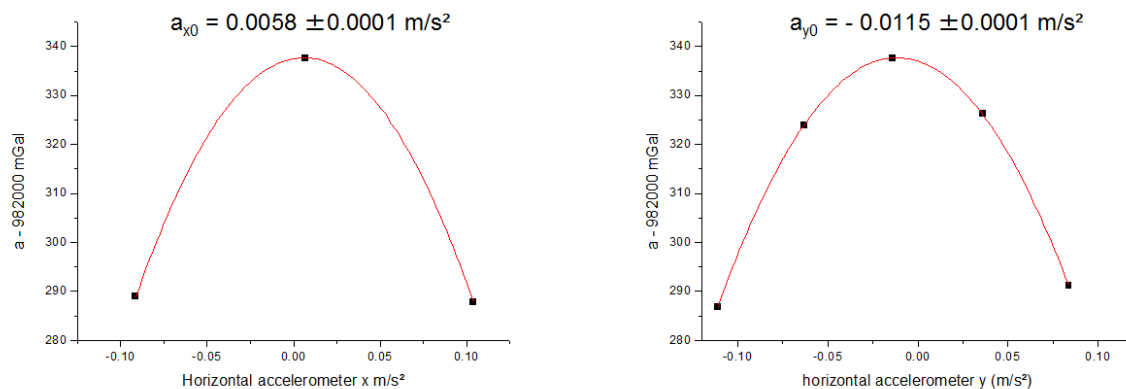
Figure 13 - Alignment of the platform, measurements of the acceleration versus the orientation of the platform. In static, the orientation of the platform is measured thanks to two horizontal accelerometers.

5.3. Airborne gravity campaign flight plan

We did five flights to test the gravimeter: one test flight to check that the gravimeter was operating well in flight and four measurements flight described on Figure 14. The first measurement flight was a straight line back and forth between Akureyri and Snaefellsjoekull. The goal of this flight is to evaluate the reproducibility of the gravity measurement. The last three measurement flights were above Vatnäjökull. The goal was here to make a gravity map of the area. The duration of each measurements flight was 3 – 4 hours.

ONERA
THE FRENCH AEROSPACE LAB
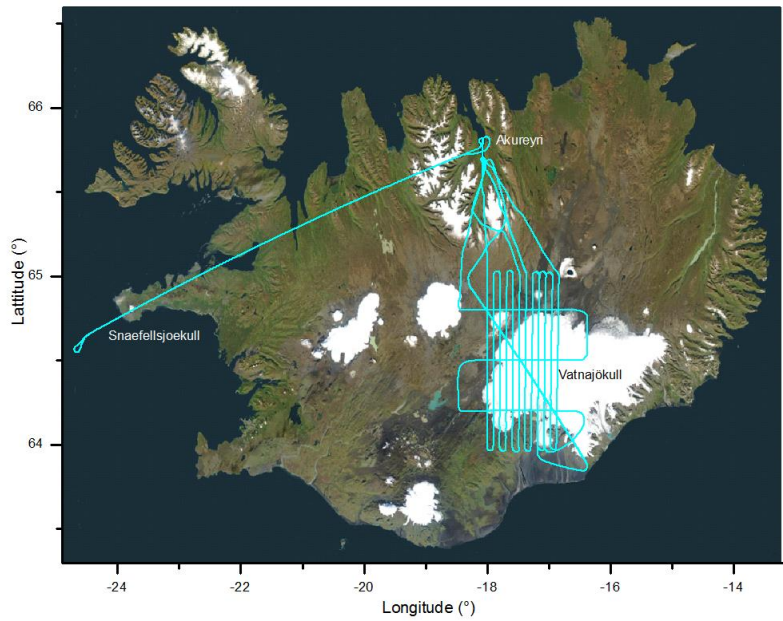
Figure 14 - Flight plans of the airborne gravity measurements.

5.4.   Flight condition

The vertical acceleration measured by the gravimeter during the flights is given on Figure 15.
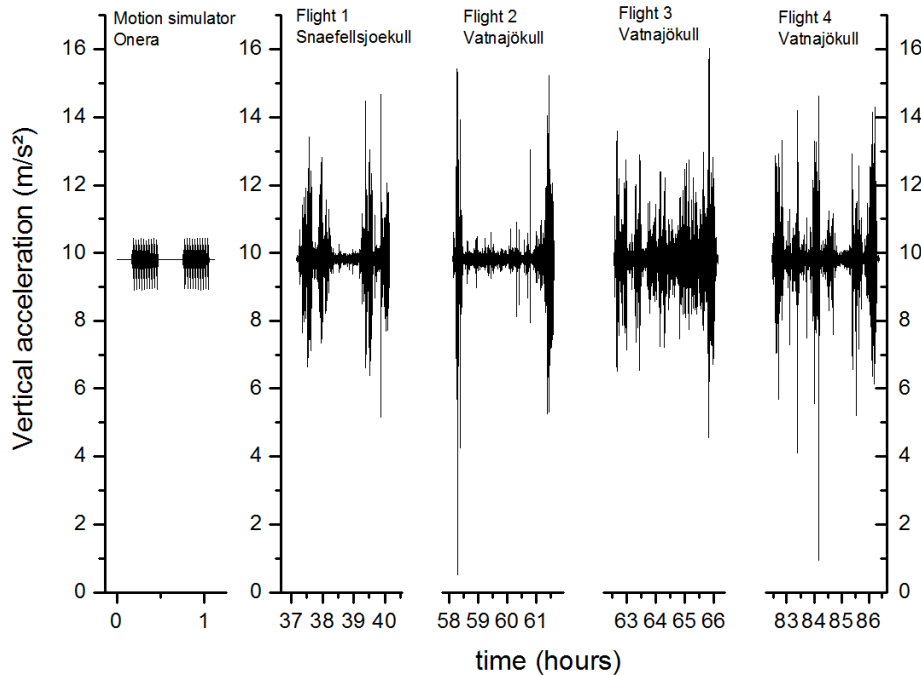
Figure 15 - Vertical acceleration measured by the gravimeter during airborne campaign.

We notice that the acceleration level during the flights is not homogeneous. During turbulent part, one can have acceleration up to 10 m/s² and during quiet part the acceleration is below 0.3 m/s². We notice also that most of the time the level of acceleration is larger than the one we simulated on the motion simulator.

ONERA
THE FRENCH AEROSPACE LAB

GEN-F157-6

6. DATA PROCESSING

6.1. Estimation of the vertical acceleration of the plane and of the Eötvös effect

The gravimeter is not only measuring the gravity acceleration but also the kinematic acceleration of the plane and the acceleration due to the coupling to Earth rotation (Eötvös effect). The acceleration measured by the gravimeter is equal to[1] :

$$a_{meas} = g + \ddot{h} + \delta g_{Eotvos}$$

Where g is the gravity acceleration, $\ddot{h}$ is second derivative of the altitude and represents the vertical kinematic acceleration of the plane, δg_{Eotvos} is the Eötvös correction which is equal to 0:

$$\delta g_{Eotvos} = -2 \cdot \omega_{Earth} \cdot \cos(\varphi) \cdot v_{East} - \frac{v_{East}^2}{N(\varphi)+h} - \frac{v_{North}^2}{M(\varphi)+h}$$

with:

$\omega_{Earth} = 7.292115.10^{-5}\ s^{-1}$	:	Earth's rotation rate
φ	:	Latitude
v_{East}	:	Velocity in the east direction
v_{North}	:	Velocity in the north direction
h	:	Altitude
$M(\varphi) = \dfrac{(a \cdot b)^2}{\left((a \cdot \cos(\varphi))^2 + (b \cdot \sin(\varphi))^2\right)^{\frac{3}{2}}}$	:	Earth's radius of curvature in the (north–south) meridian
$N(\varphi) = \dfrac{a^2}{\sqrt{(a \cdot \cos(\varphi))^2 + (b \cdot \sin(\varphi))^2}}$	:	Earth's radius of curvature in the prime vertical
a = 6 378 137.0 m	:	Earth's equatorial radius (WGS84)
b = 6 356 752.3 m	:	Earth's polar radius (WGS84)

The vertical kinematic acceleration and Eötvös effect are calculated with the GPS data (φ: latitude, λ: longitude, h: altitude) at 10 Hz (dt=0.1s) that DTU provided based on differential and post-treated DGPS data. The level arm between the GPS antenna and the gravimeter has been taking account.
The vertical kinematic acceleration, the east velocity and the north velocity have been calculated using the following equations:

$$\ddot{h}(t) = \frac{-2 \cdot h(t) + h(t+dt) + h(t-dt)}{dt^2}$$

$$v_{East}(t) = \frac{\lambda(t+dt) - \lambda(t-dt)}{2 \cdot dt} \cdot (N(\varphi)+h) \cdot \cos(\varphi)$$

$$v_{North}(t) = \frac{\varphi(t+dt) - \varphi(t-dt)}{2 \cdot dt} \cdot (M(\varphi)+h)$$

6.2. Missing data points and interpolation

The gravimeter provides acceleration measurements at a rate of 10 Hz. The precise timing of the gravimeter measurements compared to the GPS is crucial in order to correct precisely from the effect of kinematic acceleration and Eötvös effect which can be up to 10^6 times bigger than the gravity anomaly signal. However, the timing of the gravimeter measurements is not precise and has the following default:

---

[1] We use the North East Down Cartesian geographical coordinate system.

- the clock of the computer which controls the gravimeter is not precise (relative drift of $\sim 3.10^{-5}$) and has an unknown delay compared to the GPS time base;
- the recording time has a jitters compared to the real measurement time of the gravimeter;
- there are missing data points (typically 1 per hour);
- there is a 20 ms offset of the effective measurement time compared to the recording measurement time when the interrogation time of the gravimeter is changing to 10 ms.

We try to correct these limitations the best as we can the timing of the gravimeter measurement by using the following procedure. First, the missing data points are filled by inserting extrapolated measurements. Second, we assume that the measurement times of the gravimeter are given by : $t_i = i.\Delta t + T + t_0$ where $\Delta t \approx 0.1s$ is the time interval between measurements and T is the interrogation time used by the gravimeter. Then we adjust the parameter Δt and t_0 in order that the acceleration given by the GPS and the gravimeter match at the beginning and at the end of the acquisition period (see Figure 16).
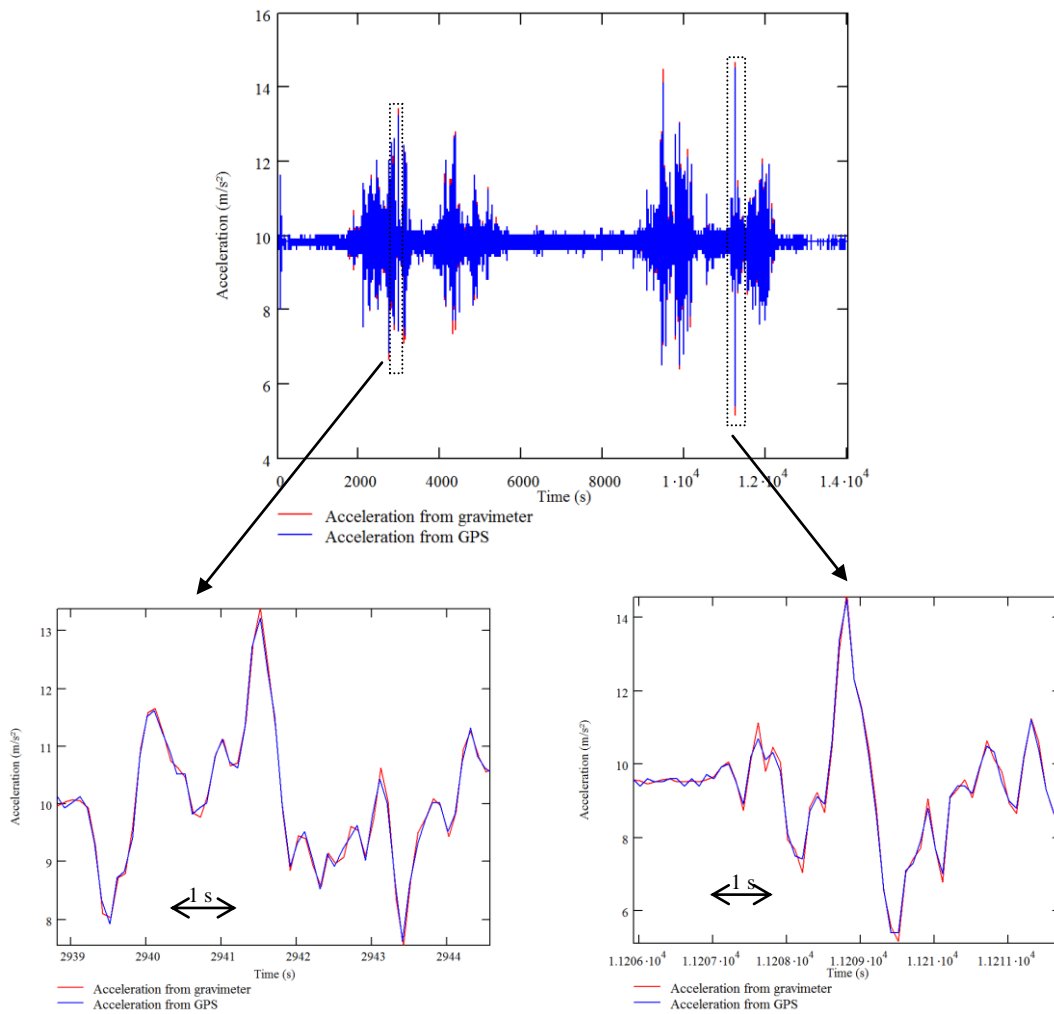
Figure 16 - Illustration of the procedure to time synchronized the GPS data and the gravity measurements.

ONERA

THE FRENCH AEROSPACE LAB

6.3.   Low pass filtering

The gravimeter measurement, the kinematic acceleration and the Eötvös correction are filtered with a 4th order Bessel low pass filter of time constant τ = 130 s. For a plane of velocity v, this gives a spatial resolution equal to 1.07·v·τ. The spatial resolution is here defined as the FWHM of the signal obtained with a Dirac input signal.

For the filter to work properly, we linearly extrapolated the gravity measurements points and the GPS data on a regular time base at 10 Hz.
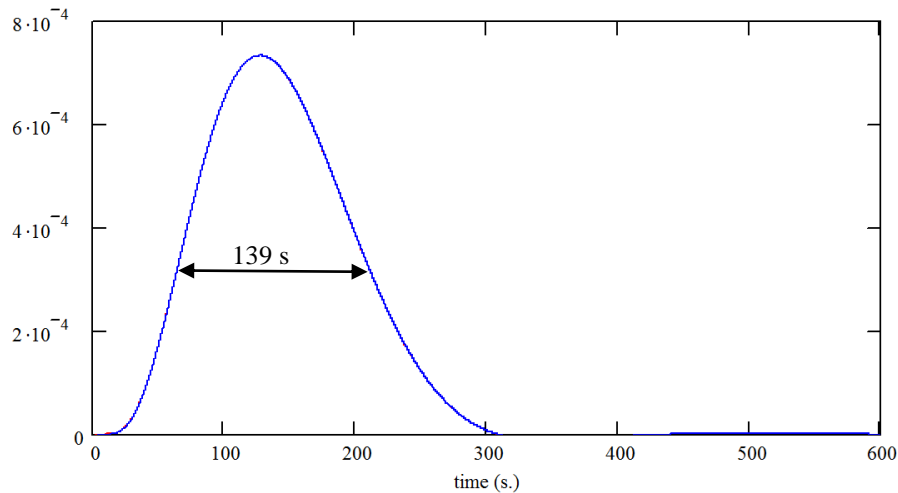
Figure 17 - Temporal response of a 4th order Bessel low pass filter with a time constant τ=130s.

6.4.   Gravity disturbance calculation

The gravity disturbance is obtained by subtracting the gravity measurement by a model of gravity taking into account altitude effect and latitude effect**Erreur ! Source du renvoi introuvable.**:

$$g_0(\varphi,h) = \frac{a \cdot g_e \cdot \cos(\varphi)^2 + b \cdot g_p \cdot \sin(\varphi)^2}{\sqrt{a^2 \cdot \cos(\varphi)^2 + b^2 \cdot \sin(\varphi)^2}} \left[1 - \frac{2}{a}\left(1 + f + \frac{a^2 \cdot b \cdot \omega_{Earth}^2}{G \cdot M_{Earth}} - 2 \cdot f \cdot \sin(\varphi)^2\right) \cdot h + \frac{3}{a^2} \cdot h^2 \right]$$

with

φ	:	Lattitude
h	:	Altitude
g_E = 9.7803253359 m/s²	:	Normal gravity at the equator
g_P = 9.8321849378 m/s²	:	Normal gravity at the pole
$G.M_{Earth}$ = 3.986004418.10^{14} m³s^{-2}	:	Gravitational constant times the mass of the Earth
Ω_{Earth} = 7.2921150 10^{-5} s^{-1}	:	Earth rotation rate
a = 6 378 137.0 m	:	Earth's equatorial radius
b = 6 356 752.3 m	:	Earth's polar radius
$f = \dfrac{a-b}{a} = \dfrac{1}{298.257223563}$	:	Flattening factor

ONERA
THE FRENCH AEROSPACE LAB

6.5. Alignment errors of the platform

Alignment errors of the platform make the gravimeter less sensitive to vertical direction and make it sensitive to horizontal acceleration. To evaluate this error, we follow the modeling approach described in the thesis of A.V. Olesen 0.

The error on gravity measurements caused by a platform misalignment is given by:

$$\delta g_{tilt} = \frac{\phi_x^{\ 2} + \phi_y^{\ 2}}{2} \cdot g + \phi_x \cdot a_x + \phi_y \cdot a_y$$

where ϕ_x and ϕ_y are the misalignment angle compared to the direction of the gravity acceleration and a_x and a_y are the horizontal acceleration. In this expression, we assume that the misalignment angles are small ($\phi_x, \phi_y \ll 1$).

The misalignment angles are estimated by comparing the measurement of the horizontal accelerometer of the sensor head and the kinematic acceleration deduced from GPS.

$$\phi_x = \frac{a_x - a_{xGPS}}{g} \qquad \phi_y = \frac{a_y - a_{yGPS}}{g}$$

with
$$a_{xGPS} = a_{EastGPS} \cdot \cos(\Phi_{yaw} + \delta\theta) - a_{NorthGPS} \cdot \sin(\Phi_{yaw} + \delta\theta)$$
$$a_{yGPS} = a_{EastGPS} \cdot \cos(\Phi_{yaw} + \delta\theta) + a_{NorthGPS} \cdot \sin(\Phi_{yaw} + \delta\theta)$$

a_x and a_y are the horizontal acceleration measured in the sensor head of the gravimeter, $a_{EastGPS}$ and $a_{NorthGPS}$ are the horizontal kinematic acceleration deduced from GPS data, Φ_{yaw} is the yaw of the plane and $\delta\theta$ is the misalignment between the axes of the gravimeter accelerometer and the yaw angle reference. This angle has been estimated equal to $\delta\theta = - 12$ mrad.

The parameter a_x, a_y, a_{xGPS} and a_{yGPS} have been pre-filtered by a 4th order Bessel filter of time resolution of 40 s (FWHM). The correction δg_{tilt} obtained has been filtered with the same filter than the gravimeter measurement i.e. a 4th order Bessel filter with a resolution of 130 s.

We obtained alignments error up to 20 mGal in period of gravity measurements i.e. constant yaw. This error is very different from flight to flight (see Table 1) and may come from initialization problem of the platform (the platform was initialized before each flight).

	δg_{tilt} max	Comments
Flight 1 : Akureyri-Snaefellsjökull	1 mGal	
Flight 2 : Vatnajökull	20 mGal	Problem of platform initialization?
Flight 3 : Vatnajökull	4 mGal	
Flight 4 : Vatnajökull	5 mGal	

Table 1 - Error on the gravity measurements due to platform misalignment.

ONERA

THE FRENCH AEROSPACE LAB

7. RESULTS

7.1. Line Akureyri-Snaefellsjökull

The measurements obtained on the line Akureyri - Snaefellsjökull flown back and forth are given on Figure 18. The plane was flying at two elevations (1900 m and 1400 m) in order to be as close as possible to the ground and thus to the gravity sources. The 1900 m altitude corresponded to mountain area and the 1400 m elevation corresponded to plain area. The velocity of the plane was 76 m/s. With the 4th order Bessel filter of time constant 130 s, one obtains a spatial resolution of 10.5 km. On the filtered acceleration graph, one can see clearly the Eötvös effect when the plane turned around. Indeed, at this point the velocity change of sign and the Eötvös effect also. On can also see clearly the effect of the vertical acceleration of the plane at the moment where the plane was changing of elevation.
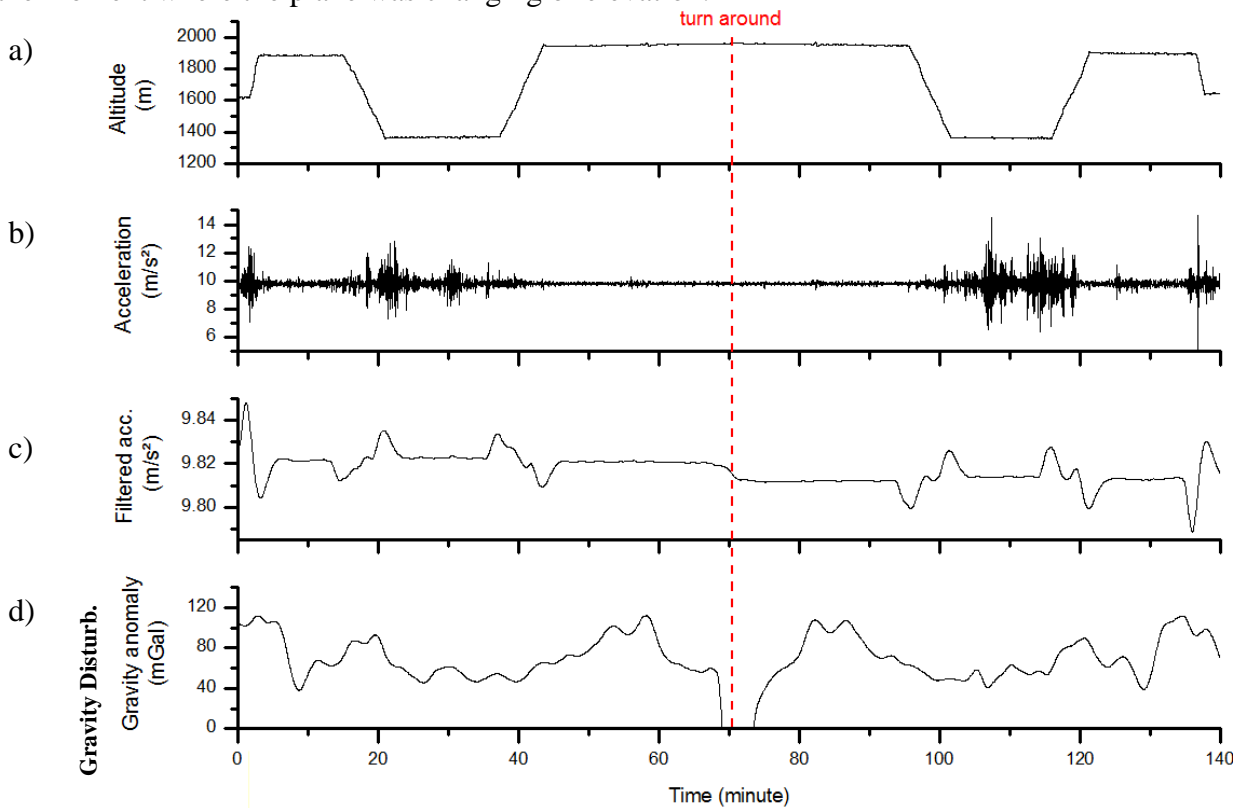
Figure 18 - Gravity measurements on the Akureyri Snaefellsjökull line. a): Altitude of the plane. b) Raw acceleration measured by the gravimeter. c) Filtered acceleration measured by the gravimeter (4th order low pass Bessel filter of time constant 130 s). d) Estimated gravity disturbance with the 130s low pass filter: $\Delta g = a_{meas} - \ddot{h} - \delta g_{Eotvos} - g_0$.

In order to estimate the repeatability of the measurements, we compared the gravity measured forward and backward (see Figure 19). The difference between forward and backward has a mean of 0.6 mGal and a standard deviation of 5.5 mGal. One notices that the big difference on the center corresponds to some missing measurement points on the gravimeter measurements. If one restricts to the area where there is no missing point, one obtains a standard deviation of 3.4 mGal close to Snaefellsjökull and 2.4 mGal close to Akureyri. Assuming uncorrelated errors between forward and backward measurements, the measurement error is given by the standard deviation of the difference divided by $\sqrt{2}$. One obtains thus an estimated error ranging from 1.7 mGal to 3.9 mGal depending on the area considered.

ONERA

THE FRENCH AEROSPACE LAB
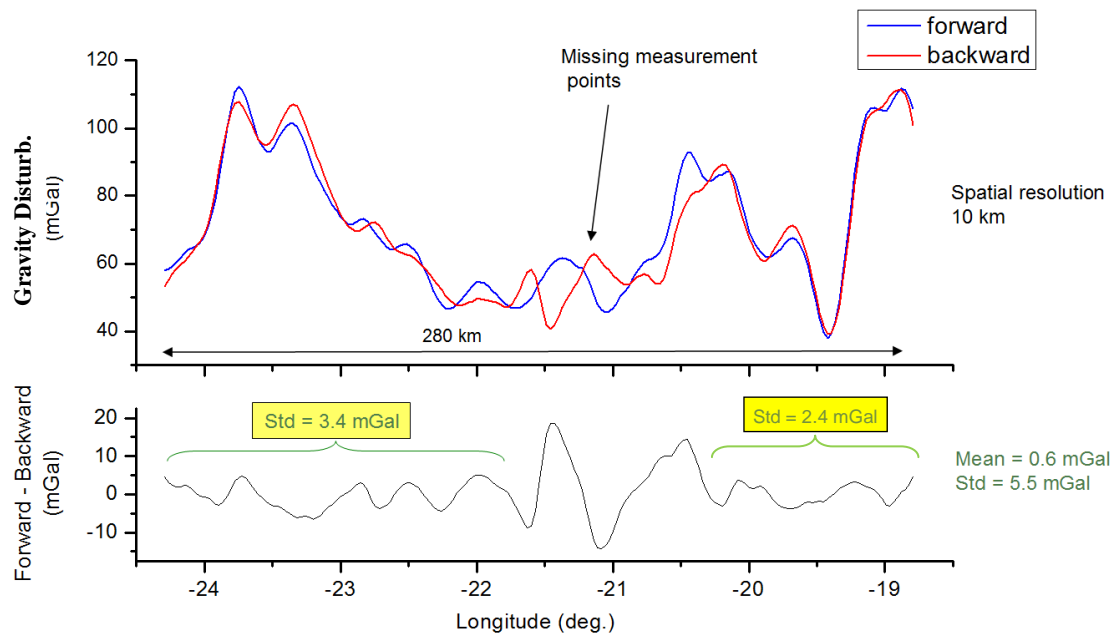
Figure 19 – Comparison of the gravity measurement along the line Akureyri- Snaefellsjökull for the forward and backward flight.

7.2. Gravity measurements above Vatnajökull

During three flights, we measured gravity above the area of Vatnajökull along 16 lines. The gravity disturbance measurements obtained are reported on Figure 20. One notices two measurements area missing which correspond to moments where the gravimeter was not operational due to laser misalignment.
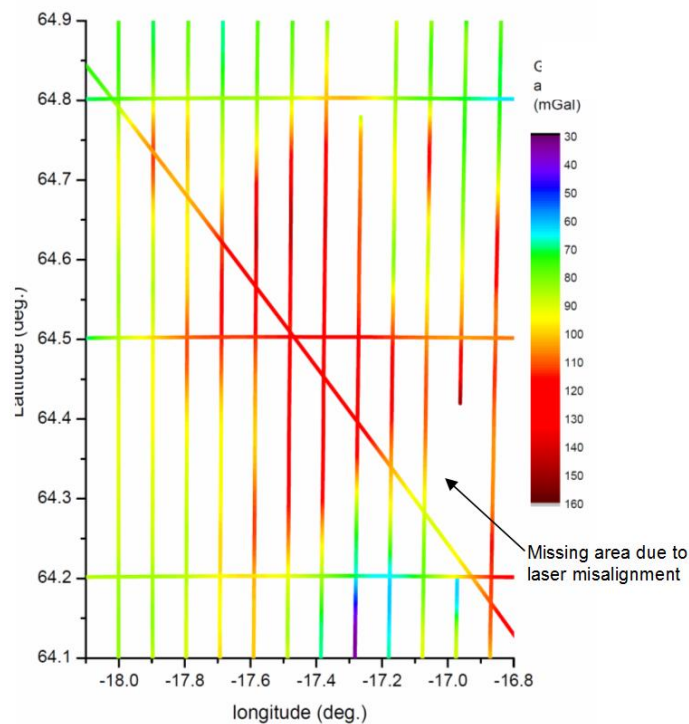
Figure 20 - Gravity measurements above Vatnajökull.

ONERA
THE FRENCH AEROSPACE LAB

The differences at the crossings points of the survey are reported on Figure 21. One obtains a standard deviation of 2.4 mGal on the difference. Assuming no correlation, one can estimate a measurement error of 1.7 mGal (std/$\sqrt{2}$).
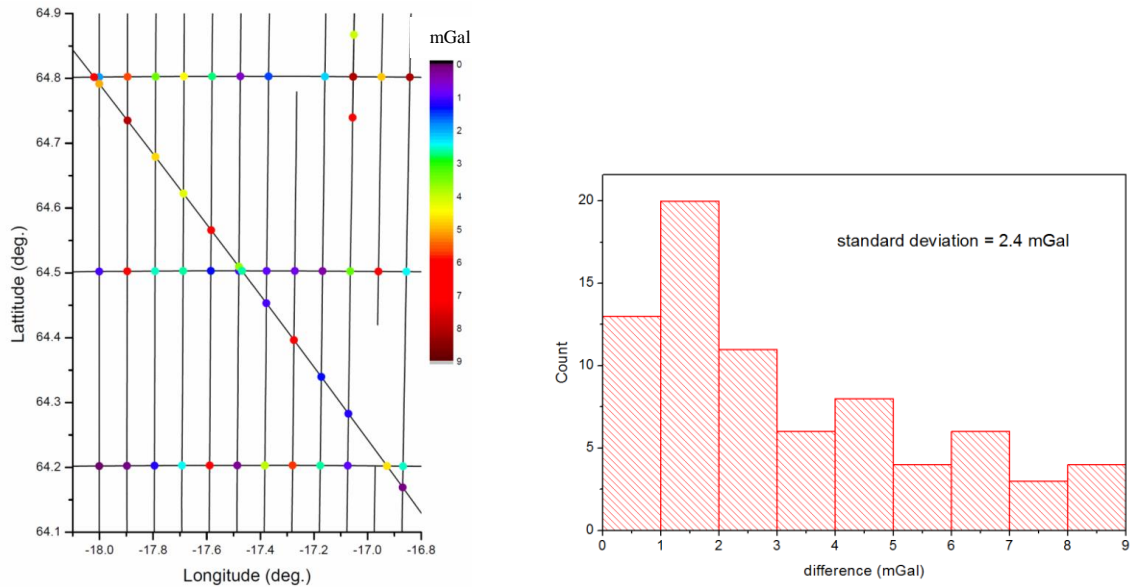
Figure 21 - Difference at the crossing points for the Vatnajökull survey.

A gravity model of the measurements area has been computed using a 2D polynomial fit of the measurements. A polynomial of order 12 has been used for the fit. A polynomial of higher order conduct to divergence in the area where there is no measurements.
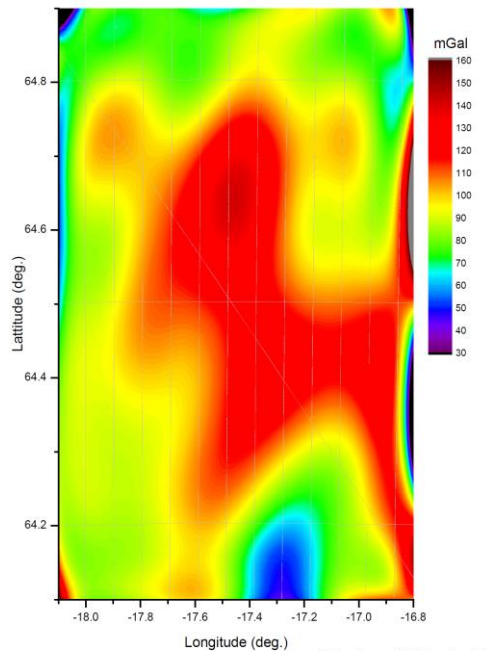
Figure 22 - Model of gravity in the Vatnajökull area obtained by a 2D polynomial fit (order12) of the measurement.

ONERA
THE FRENCH AEROSPACE LAB

7.3.   DTU data processing and comparison with ground truth

The Iceland region has a relatively dense ground gravity coverage, as shown in Figure 23. The use of upward continued surface gravimetry represent an independent validation opportunity for the cold atoms gravimetry results, especially important due to the failure of the flown DTU iMAR strapdown gravimetry unit (due to a faulty upgrade at the iMAR factory shortly before the field campaign, without possibility for testing ahead of the campaign). The Iceland gravity data were surveyed primarily in the 1980's, and provided by Landmælingar Islands (Iceland Geodetic Survey).
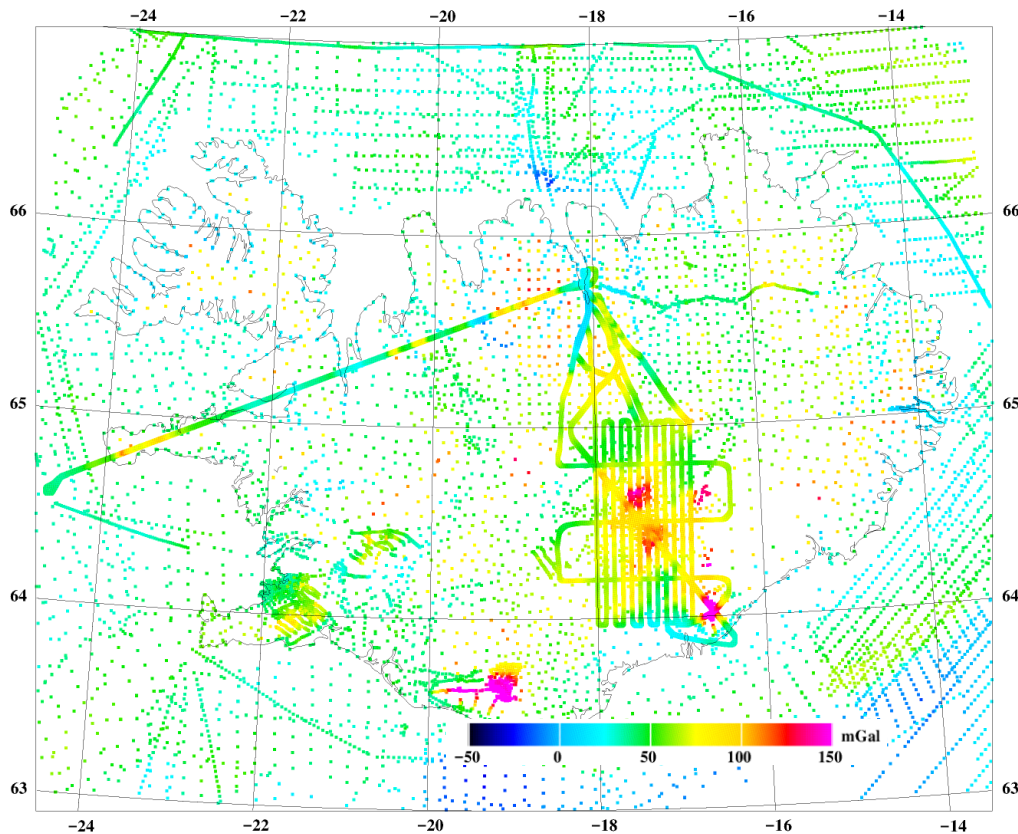
Figure 23 - Iceland gravity coverage, overlaid with the cold atom gravimetry results. The positive free-air anomalies shown are predominantly due to volcanoes under the ice caps, and topographic highs.

The upward continuation estimation of the free-air anomalies at altitude were done using the GRAVSOFT suite of programs [41], using standard remove-restore techniques of physical geodesy (use of EGM2008 as reference field, integration of terrain effects by prism integration, and upward continuation to the flight altitude by Fast Fourier transform methods [42]). A digital terrain model at 200 m resolution was used, cf. Figure 24, and combined with an ice cap thickness model of the 3 main ice caps in Iceland (including Vatnajökull), derived from radar echo soundingand. also provided by Landmalinger Islands, as part of cooperation on geoid determination.

ONERA

THE FRENCH AEROSPACE LAB
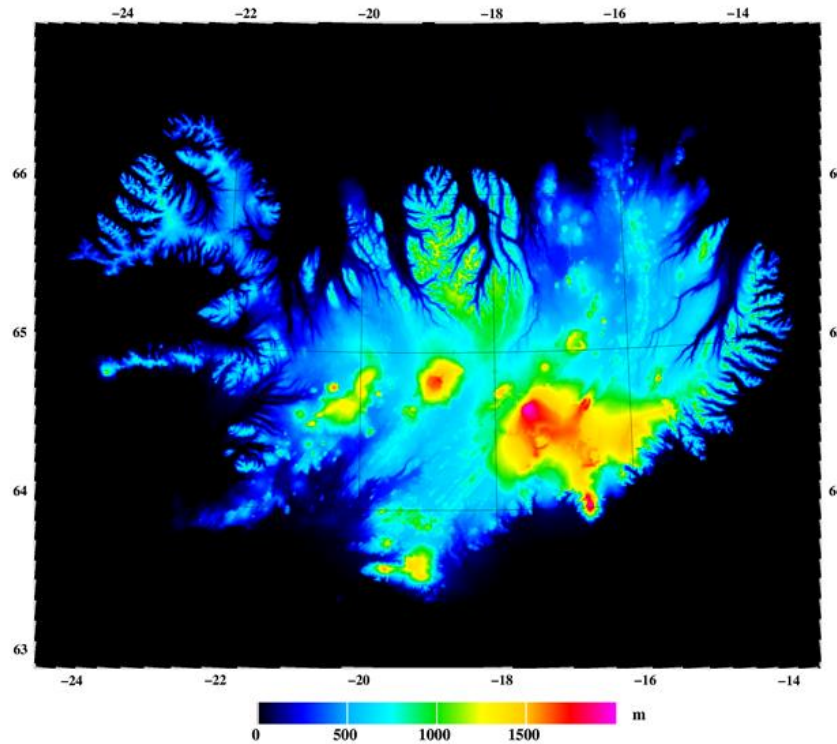
Figure 24 - *The Iceland digital elevation model, used for the upward continuation of the ground data.*

The predicted versus the observed cold atom gravimetry results are shown in Figure 26 and Figure 25 below, with the predicted data at altitude are filtered with a similar 4th order Bessel filter with time constant 130 s, to match the airborne data filter. One notices that similar gravity signals are obtained with the two models confirming the relevance of the cold atom gravimeter measurements.

For Vatnajökull flights, we noticed that in some areas (see Figure 25), the difference between airborne and ground is large. This areas correspond to the beginning of a track (after a plane turn), to a period around laser misalignment problem and to a severe turbulence period. If we removed this areas, the standard deviation becomes two times smaller (see Table 2).

ONERA
THE FRENCH AEROSPACE LAB
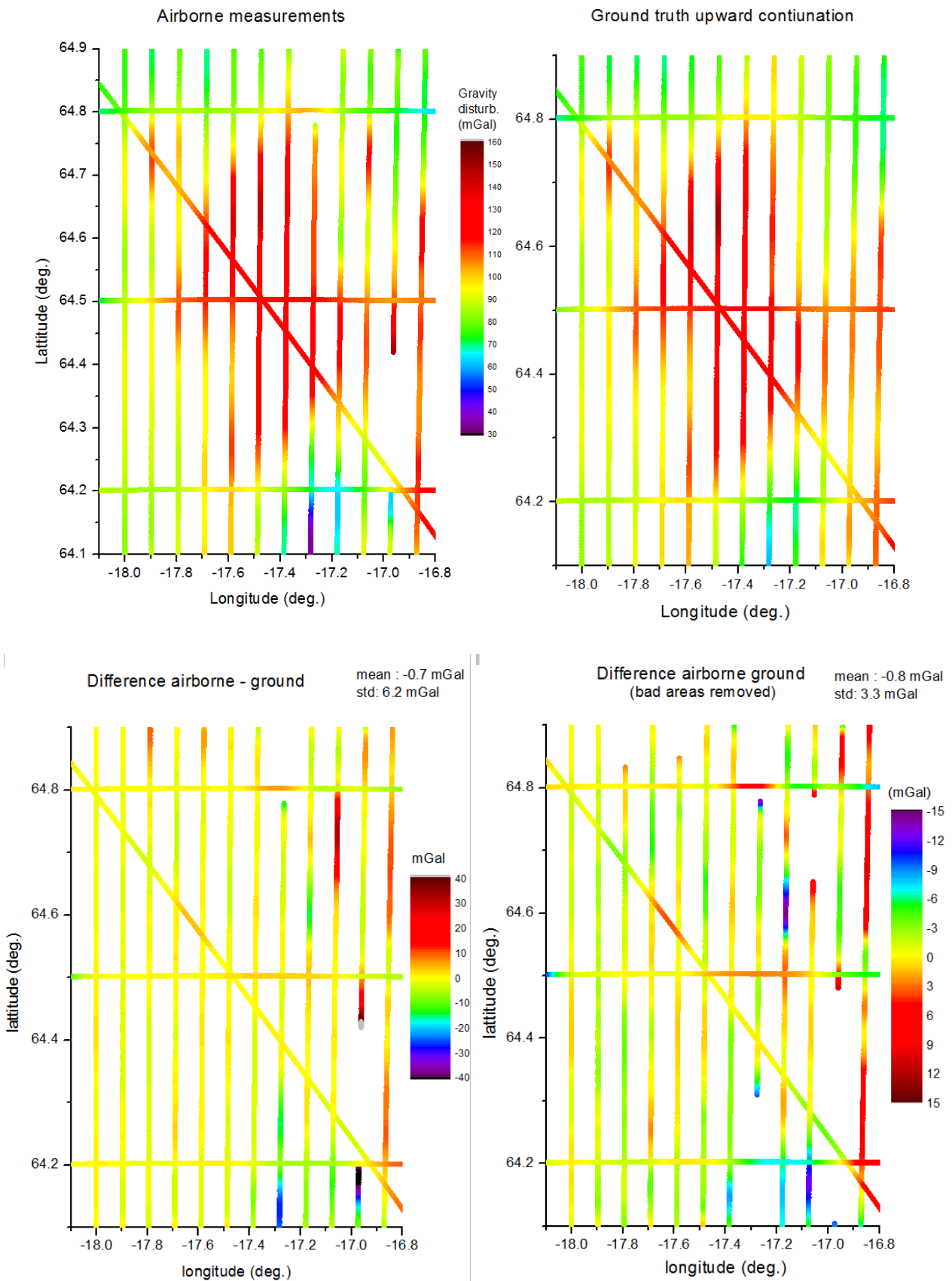
Figure 25 - Comparison between airborne measurements and ground measurements upward continued above Vatnajökull.
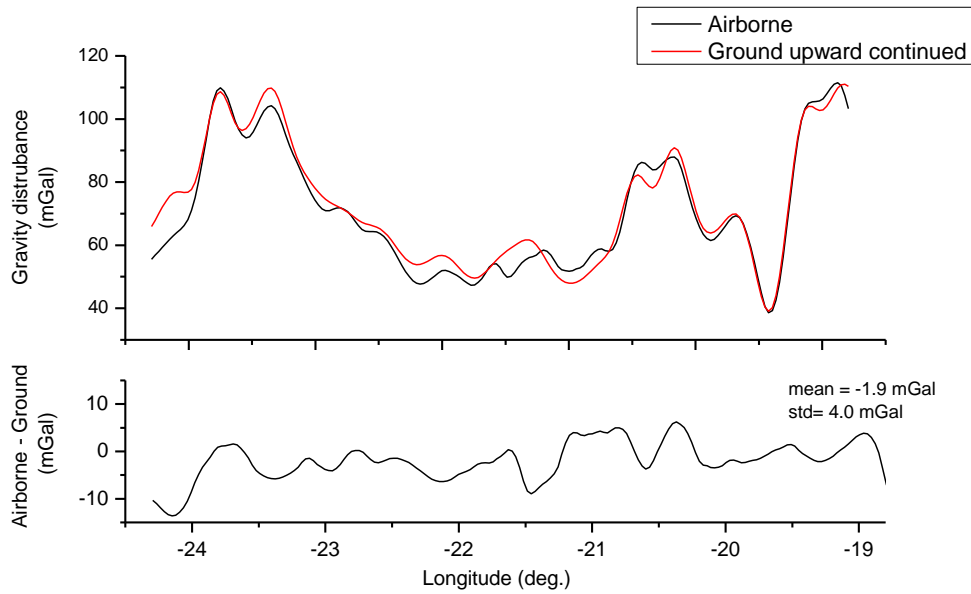
spatial resolution = 10 km

Figure 26 – Comparison between airborne measurement and ground measurement upward continued on the the line Akureyri-Snaefellsjökull

Statistics (mGal)	Mean	Standard deviation
Akureyri- Snaefellsjökull	-1.9	4.0
Vatnajökull	-0.7	6.2
Vatnajökull (bad area removed)	-0.8	3.3

Table 2 – Statistics on the difference between airborne and ground upward continued gravity measurements

The airborne data comparison in Figure 25 is showing some differences in the eastern tracks, likely due to severe turbulence. An issue for the comparison of surface and airborne data is also the possible geodynamic gravity changes between the surface and airborne gravity epochs, since several volcanic eruptions have taken plane, especially the Bardabunga eruption of 2014, which had major dyke intrusion activity in the northwestern region of the Vatnajökull ice cap.

ONERA
THE FRENCH AEROSPACE LAB

8. CONCLUSION

In conclusion, we demonstrated for the first time airborne gravity measurements and survey with a cold atom sensor. The main advantage of this technology is that it provides absolute measurements (no drift and no calibration needed). The precision of the gravity measurements have been estimated thanks to comparison on a forward and backward line and to differences at crossing points. Measurement errors ranging from 2 to 4 mGal have been obtained. The airborne gravity measurements have been also compared to upward continued ground truth. The standard deviation on the difference is ranging from 3 to 6 mGal.

This is a promising result for a sensor designed for marine application. This campaign gave us also the technological improvements needed for a future dedicated airborne cold atom gravimeter with better precision, reliability and operationality:
- measurements points on a regular time basis (GPS dating) with no missing measurement points;
- replacement of the frequency doubled optical bench by a fiber bench (to solve lase misalignement);
- optimization of hybridization algorithm for airborne environment;
- optimization of the gyro-stabilized platform for airborne environment;
- lower electrical consumption;
- decrease the size of the control cabinet (electronic, optics).

Other gravity campaigns will be necessary to test these improvements and continue the developments of the cold atom gravimeter. The prototype tested in this campaign is dedicated to marine application. The building of dedicated airborne prototype will be necessary to continue this development and to do regular airborne gravity campaigns.

With cold atom technology, we should obtain sub-mGal absolute airborne gravity measurements with a reliable sensor easy to use in an airplane. This instrument should lead to a breakthrough in the field of geodesy.
Finally, these results show the maturity of cold atom technology for onboard application and support the development of cold atom sensor for measuring the Earth gravity field from space [40].

9. ACKNOWLEDGEMENTS

ONERA
THE FRENCH AEROSPACE LAB

10.   REFERENCES

[1] Sandwell, D.T., Dietmar Müller R., Smith W.H.F., Garcia E. & Francis R.
New global marine gravity model from CryoSat-2 and Jason-1 reveals buried tectonic structure.
Science **346**, 65-67 (2014).

[2]   Carbone D., Zuccarello L., Messina A., Scollo S. & Rymer H.
Balancing bulk gas accumulation and gas output before and during lava fountaining episodes at Mt. Etna.
 Sci. Rep. **5**, 18049 (2015).

[3] Montagner, J. P. et al.
Prompt gravity signal induced by the 2011 Tohoku-Oki earthquake.
Nat. Commun. **7**, 13349 (2016).

[4] Velicogna, I. & Wahr, J.
Measurements of Time-Variable Gravity Show Mass Loss in Antarctica.
Science **311**, 1754-1756 (2006).

[5] Reager J. T., Thomas, B. F. & Famiglietti, J. S.
River basin flood potential inferred using GRACE gravity observations at several months lead time.
Nat. Geosci. **7**, 588–592 (2014).

[6] Nabighian, M. N. et al.
Historical development of the gravity method in exploration.
Geophysics **70**, 63ND (2005).

[7] Chatfield, A. B.
Fundamentals of High Accuracy Inertial Navigation.
Prog. Aerosp. Sci. **174,** 291-304 (1997).

[8] Tapley, B. D., Bettadpur, S., Watkins, M. & Reigber C.
The Gravity Recovery and Climate Experiment: Mission overview and early results.
 Geophys. Res. Lett. **31**, L09607 (2004).

[9] Tapley, B. D., Bettadpur, S., Ries, J. C., Thompson, P. F., Watkins, M. M.,
GRACE Measurements of Mass Variability in the Earth System.
 Science 305, 503-505 (2004).

[10] Bouman, J., Ebbing, J., Fuchs, M., Sebera, J. & Lieb, V.
Satellite gravity gradient grids for geophysics.
Sci. Rep. **6**, 21050 (2016).

ONERA

THE FRENCH AEROSPACE LAB

[11] Pail, R. et al.
First GOCE gravity field models derived by three different approaches.
J. Geod. **85**, 819–843 (2011).

[12] Baumann, H., Klingelé, E. & Marson I.
Absolute airborne gravimetry: a feasibility study.
Geophysical Prospecting **60**, 361-372 (2012).

[13] Berman, P. R.
Atom interferometry.
(Acad. Press, 1997).

[14] Hamilton, P. et al.
Atom-interferometry constraints on dark energy.
Science **349**, 849-851 (2015).

[15] Kovachy, T. et al.
Quantum superposition at the half-metre scale.
Nature **528**, 530-533 (2015).

[16] Rosi, G., Sorrentino, F., Cacciapuoti, L., Prevedelli, M. & Tino, G.M.
Precision measurement of the Newtonian gravitational constant using cold atoms.
Nature **510**, 518–521 (2014).

[17] Bouchendira, R., Cladé, P., Guellati-Khélifa, S., Nez, F. & Biraben, F.
New Determination of the Fine Structure Constant and Test of the Quantum Electrodynamics.
Phys. Rev. Lett. **106**, 080801 (2011).

[18] Peters, A., Yeow Chung, K. & Chu, S.
Measurement of gravitational acceleration by dropping atoms.
Nature **400**, 849 – 852 (1999).

[19] Gillot, P., Francis, O., Landragin, A., Pereira Dos Santos, F. & Merlet S.
Stability comparison of two absolute gravimeters: optical versus atomic interferometers.
Metrologia **51**, L15–L17 (2014).

[20] Freier, C. et al.
Mobile quantum gravity sensor with unprecedented stability.
J. Phys. Conf. Ser. **723**, 012050 (2016).

[21] Hu, Z.-K. et al.
Demonstration of an ultrahigh-sensitivity atom-interferometry absolute gravimeter.
Phys. Rev. *A* **88**, 043610 (2013).

[22] McGuirk, J. M., Foster G. T., Fixler, J. B., Snadden, M. J., & Kasevich, M. A.
Sensitive absolute-gravity gradiometry using atom interferometry.
Phys. Rev. A **65**, 033608 (2002).

ONERA
THE FRENCH AEROSPACE LAB

[23] Sorrentino, F. et al.
Sensitivity limits of a Raman atom interferometer as a gravity gradiometer.
Phys. Rev. A **89**, 023607 (2014).

[24] Berg, P. et al.
Composite-Light-Pulse Technique for High-Precision Atom Interferometry.
Phys. Rev. Lett. **114**, 063002 (2015).

[25] Dutta, I. et al.
Continuous Cold-Atom Inertial Sensor with 1 nrad/sec Rotation Stability.
Phys. Rev. Lett. **116**, 183003 (2016).

[26] Durfee, D. S., Shaham, Y. K. & Kasevich, M. A.
Long-term stability of an areareversibleatom-interferometer sagnac gyroscope
Phys. Rev. Lett. 97, 240801(2006).

[27] Mahadeswaraswamy, C.
Atom interferometric gravity gradiometer: disturbance compensation and mobile gradiometry,
PhD thesis, Stanford University (2009).

[28] Bidel, Y. et al.
Compact cold atom gravimeter for field applications.
Appl. Phys. Lett. **102**, 144107 (2013).

[29] Geiger, R. et al.
Detecting inertial effects with airborne matter-wave interferometry.
Nat. Commun. **2**, 474 (2011).

[30] Barrett, B. et al.
Dual matter-wave inertial sensors in weightlessness.
Nat. Commun. **7**, 13786 (2016).

[31] Müntinga, H. et al.
Interferometry with Bose-Einstein Condensates in Microgravity.
Phys. Rev. Lett. **110**, 093602 (2013).

[32] MAIUS 1 – *First Bose-Einstein condensate generated in space*.
http://www.dlr.de/dlr/en/desktopdefault.aspx/tabid-10081/151_read-20337/#/gallery/25194
(2017).

[33] Bidel, Y. et al.
Absolute marine gravimetry with matter-waveinterferometry
Nat. Commun. **9**, 627 (2018).

ONERA
THE FRENCH AEROSPACE LAB

[34] Carraz, O. et al.
Phase shift in an atom interferometer induced by the additional laser lines of a Raman laser generated by modulation.
Phys. Rev. A **86**, 033605 (2012).

[35] Merlet, S. et al.
Operating an atom interferometer beyond its linear range.
Metrologia **46**, 87–94 (2009).

[36] Lautier, J. et al.
Hybridizing matter-wave and classical accelerometers.
Appl. Phys. Lett. **105**, 144102 (2014).

[37] Carraz, O. et al.
Compact and robust laser system for onboard atom interferometry.
Appl. Phys. B **97**, 405–411 (2009).

[38] Olesen, A. V.

Improved airborne scalar gravimetry for regional gravity field mapping and geoid determination,
PhD Thesis, University of Copenhagen (2002).

[39] Torge, W.
Gravimetry.
W. de Gruyter, 1989

[40] Carraz, O., Siemes, C., Massotti, L., Haagmans, R. & Silvestrin, P.,
A spaceborne gravity gradiometer concept based on cold atom interferometers for measuring Earth's gravity field.
Microgravity Sci. Technol. **26**, 139-145 (2014).

[41] Tscherning, C. C., R. Forsberg and P. Knudsen
The GRAVSOFT package for geoid determination.
Proc. IAG first continental workshop for the geoid in Europe, Praque, pp. 327-334, 1992.

[42] Schwarz, K. P., M. G. Sideris, R. Forsberg
Use of FFT methods in Physical Geodesy.
Geophysical Journal International, vol. 100, pp. 485 514, 1990.

ONERA
THE FRENCH AEROSPACE LAB

The "cold atoms"campaign field team: From left to right: N. Zahzam (ONERA), A. Olesen (DTU), A. Bresson (ONERA), Y. Bidel (ONERA), G. Valsson (Landmælingar Islands) and R. Forsberg (DTU).

ONERA
THE FRENCH AEROSPACE LAB